THE ASTROPHYSICAL JOURNAL, 374:212–217, 1991 June 10

A NEW LOOK AT THE "JET" IN THE CTB 37A/B SUPERNOVA REMNANT COMPLEX

NAMIR E. KASSIM,[1] STEFI A. BAUM,[2,3] AND KURT W. WEILER[1]

Received 1990 September 27; accepted 1990 December 5

ABSTRACT

Very Large Array observations of the unusual southern Galactic supernova remnant (SNR) complex near $l = 348°$, $b = 0°$ at wavelengths of 6, 20, and 90 cm are presented. Derived continuum spectra and observed morphologies indicate that G348.5+0.1 (CTB 37A) does not have a "jet" as reported by previous observers but is instead superposed on a second, previously unidentified SNR lying along the line of sight. This new SNR is designated G348.5−0.0 according to the usual convention. Other observers have also noted a faint, flat spectrum bridge of emission possibly connecting the G348.5+0.1/G348.5−0.0 superposition with a third nearby remnant G348.7+0.3 (CTB 37B). However, a connection appears unlikely, and we suggest that the "bridge" merely consists of faint emission which has "leaked" from the southeastern side of G348.7+0.3 and has no relation to the G348.5+0.1/G348.5−0.0 superposition.

These new data also reveal a remarkable region of "blown-out" emission from the southwestern part of G348.5+0.1 which most likely reflects the presence of large-scale density inhomogeneities in the interstellar medium into which the SNR shell is expanding.

Subject headings: nebulae: individual (G348+0) — nebulae: structure — nebulae: supernova remnants

1. INTRODUCTION

Milne et al. (1979) and Downes (1984) have reviewed radio observations of the unusual Galactic supernova remnants (SNRs) CTB 37A (hereafter G348.5+0.1) and CTB 37B (hereafter G348.7+0.3) made over a wide range of frequencies. Milne et al. (1979) note an apparent "jet" feature aligned perpendicular to and appearing to "emerge" from the eastern side of G348.5+0.1 and a "bridge" of flat spectrum radio emission which appears to connect G348.5+0.1 with G348.7+0.3. The latter remnant lies to the north of the former, and they are separated by a distance roughly comparable to their diameters (~15′). The possibility of a physical connection between the two SNRs is enhanced by H I absorption measurements to both remnants, albeit with large associated errors, which indicate similar distance estimates of 10.2±3.5 kpc (Green 1988). The observations by Downes (1984) confirm the general morphology reported by Milne et al. (1979) and also reveal lower surface brightness emission associated with the "jet" and "bridge." Downes (1984) notes that this emission would strengthen the case for the "jet" being part of a third SNR in the complex, a suggestion explored and rejected by Milne et al. (1979).

In the course of very low frequency observations (57.5 MHz) made while conducting the Clark Lake Radio Observatory (CLRO) Galactic Plane Survey (Kassim 1987, 1988), Kassim (1987) noted that the combined flux density of G348.5+0.1 and G348.7+0.3, which are not resolved at the CLRO resolution, exceeds the expected flux density extrapolated from higher frequencies by more than a factor of 2. This fact, together with the unusual morphology of the complex, motivated us to observe this unusual field at higher resolution. We therefore obtained observations of the complex with the Very Large Array (VLA)[4] at 90, 20, and 6 cm wavelengths. Our new 90 cm data have enabled us to establish flux densities for all sources in the field which, when combined with previous observations from the literature, allows the derivation of continuum spectra for all features. Combination of these spectra with the morphology revealed by our higher resolution VLA observations permits a reinterpretation of the structure of the region and the identification of a new SNR, G348.5−0.0.

2. OBSERVATIONS

The complex region containing G348.5+0.1 and G348.7+0.3 was observed at 90, 20, and 6 cm wavelength in the B/C hybrid array of the VLA on 1986 September 27 and in the C/D hybrid on 1987 February 8. These observations are summarized in Table 1. Because of the southern declination of the region, maximum resolution was achieved by using the B/C hybrid, and maximum sensitivity to large scale structure was achieved by using the C/D hybrid. The resulting synthesized beams at each wavelength have full width at half-maximum (FWHM) of 53″ × 46″ at position angle +30° for 90 cm, 33″ × 18″ at position angle +5° for 20 cm, and 3.″9 × 2.″5 at position angle +32° for 6 cm.

Calibration at 6, 20, and 90 cm used short observations of the primary calibrator 3C 286, defined to have flux densities of 7.420, 14.620, and 26.77 Jy at 6, 20, and 90 cm, respectively, to determine the flux densities of possibly variable secondary calibrators 1602+01 (at 20 cm), 1827−360 (at 90 and 20 cm), and 1921−293 (at 6 cm) at each epoch of observation. Then, observations of these secondary calibrators, which are compact with well-determined positions, were used to calibrate the phase and gain of the instrument for each observation of the SNRs. Standard computer programs were used to interpolate the gain and phase of the instrument between calibrator observations. These procedures are normal for the VLA and are thought to provide a flux density calibration which is consistent to a few

[1] NRL-Code 4215.3, Center for Advanced Space Sensing, Naval Research Laboratory, Washington, DC 20375-5000.
[2] Also Hubble Research Fellow at Johns Hopkins University.
[3] Postal address: Radiosterrenwacht Dwingeloo, Postbut 2, 7990 AA Dwingeloo, The Netherlands.

[4] The VLA is a facility of the National Radio Astronomy Observatory operated by Associated Universities Inc., under a cooperative agreement with the National Science Foundation.

TABLE 1

SUMMARY OF OBSERVATIONS

VLA Configuration	Center Frequency (MHz)	Wavelength (cm)	Bandwidth (MHz)	Integration Time (minutes)	Date Observed
B/C	4823	6	50	20	1986 Sep 27
	4885	6	50	23	1986 Sep 27
	1443	20	50	211	1986 Sep 27
	333	90	3	211	1986 Sep 27
C/D.....	4823	6	50	27	1987 Feb 8
	4885	6	50	27	1987 Feb 8
	1443	20	50	183	1987 Feb 8
	333	90	3	210	1987 Feb 8

percent with possible systematic errors of up to ~5% at each wavelength. For a more detailed description of the VLA see Napier, Thompson, & Ekers (1983).

The shortest array spacings at 6, 20, and 90 cm were ~500λ, 200λ, and 40λ, respectively. This means that sources larger than ~5′ at 6 cm, ~15′ at 20 cm, and ~90′ at 90 cm may be undersampled and have their flux densities underestimated. The individual data sets, after calibration, correction, and inspection for quality, were added to produce a single data set for each observing wavelength. These were then Fourier-inverted to produce initial maps. These "dirty maps" were self-calibrated, CLEANed, and restored with elliptical gaussian beams. The final maps, after correction for primary beam attenuation, are shown in Figure 1 (90 cm), Figure 2 (20 cm), and Figure 3 (6 cm). The measured rms noise levels are ~50 mJy beam^{-1} on the 90 cm map, ~10 mJy beam^{-1} on the 20 cm map, and ~0.7 mJy beam^{-1} on the 6 cm map.

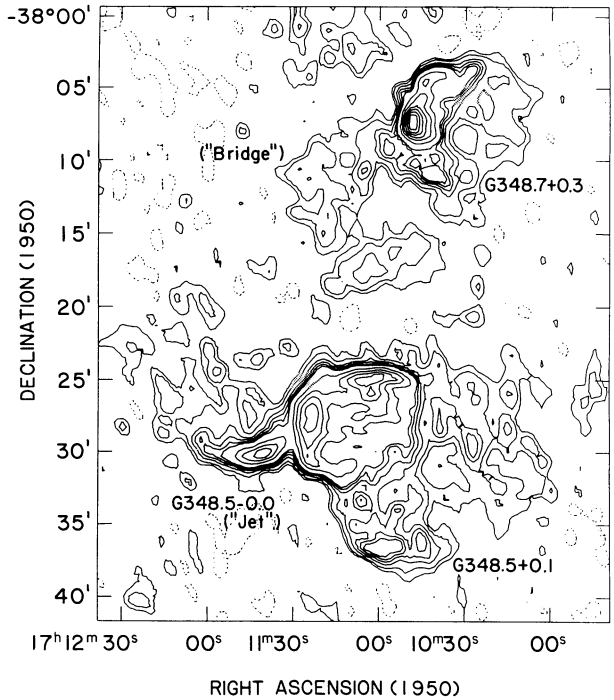

FIG. 1.—90 cm map of the G348+0 SNR complex made from data taken in the B/C and C/D hybrid configurations of the VLA. The synthesized FWHM beamwidth is 53″ × 46″ at position angle +30°. The contour levels are (−2, 1, 2, 4, 6, 8, 10, 20, 30, 40, 50, 60, 70, 80, 90, 100, 120, 140) × 50 mJy beam^{-1} with a peak brightness of 7.71 Jy beam^{-1}.

3. RESULTS

3.1. 90 *Centimeter Observations*

Our 90 cm map (Fig. 1) has the largest field of view (antenna primary beam size 156′ FWHP) and is thus the only map which shows all sources in the G348+0 complex. The resolution of the 90 cm map is similar to that used by other observers, and we reproduce the 1415 MHz FST map of Milne et al. (1979) in Figure 4 (resolution 54″ × 47″) for comparison purposes. While comparison of Figures 1 and 4 shows many similarities in the gross structures, a number of important differences are worth noting:

1. Our 90 cm map (Fig. 1) shows emission from the western part of G348.7+0.3 which is not detected by Milne et al. (1979).

2. The 90 cm map reveals low surface brightness emission near $\alpha = 17^h11^m15^s$, $\delta = -38°12'$ (not detected in the FST map) which connects the "bridge" with the southwestern part of G348.7+0.3; thus the "bridge" of emission "between" G348.7+0.3 and G348.5+0.1 appears unrelated to the latter SNR and is probably only a faint extension of the former; henceforth, we consider it part of the SNR G348.7+0.3.

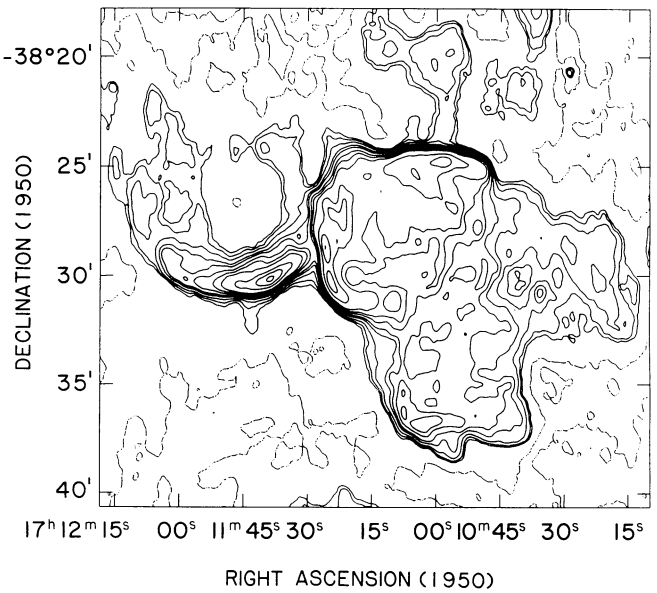

FIG. 2.—20 cm VLA map of G348.5+0.1 and G348.5−0.0 (formerly the "jet") taken with the same array configuration as in Fig. 1. The synthesized FWHM beamwidth is 33″ × 18″ at position angle +5°. The contour levels are at (−20, −10, 2.5, 5, 10, 20, 30, 50, 70, 100, 200, 300, 400) × 1 mJy beam^{-1} with a peak brightness of 427 mJy beam^{-1}.

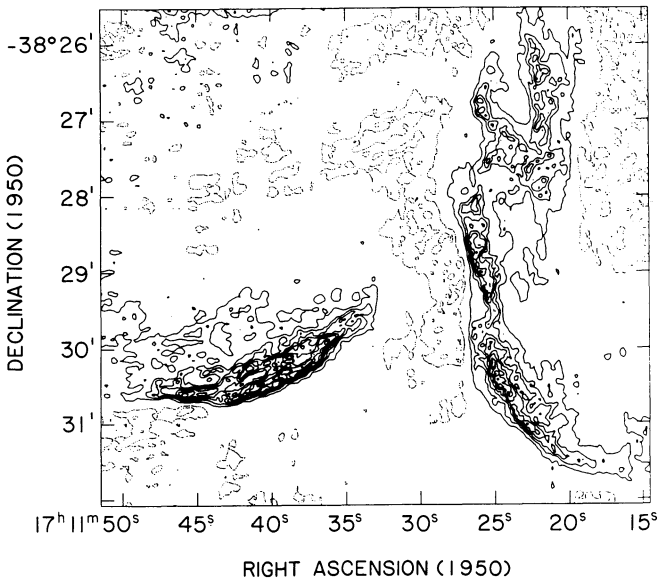

FIG. 3.—6 cm VLA map of the eastern edge of G348.5+0.1 and G348.5−0.0 (formerly the "jet") taken with the same array configuration as in Fig. 1. The synthesized FWHM beamwidth is 3.″9 × 2.″5 at position angle +32°. The contour levels are at (−2, −1, 1, 2, 3, 4, 5, 6, 7, 8, 9, 10) × 1 mJy beam^{-1} with a peak brightness of 12.0 mJy beam^{-1}.

3. G348.5+0.1 has a much larger region of faint extended emission to the southwest than is apparent on the FST 1415 MHz map. (Note, however, that evidence for this extension does appear in some earlier work such as Culgoora at 80 MHz, Molonglo at 408 MHz, and Parkes at 14.7 GHz—see Milne et al. 1979).

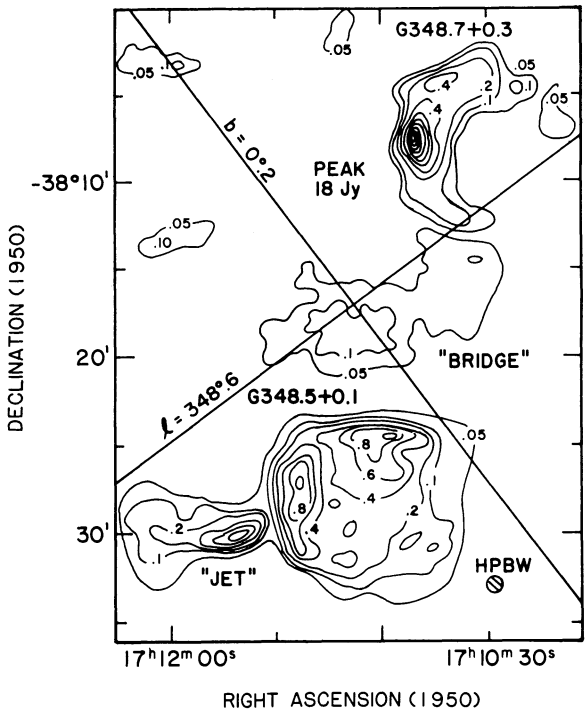

FIG. 4.—20 cm FST map of the G348+0 SNR complex by Milne et al. (1979). Synthesized FWHM beamwidth of 54″ × 47″ is almost identical to that of our 90 cm observations shown in Fig. 1. The contours are labeled in units of Jy beam^{-1}.

4. The "jet" feature is prominent on both the FST 1415 MHz and VLA 90 cm maps and is aligned nearly perpendicular to the eastern side of the shell of G348.5+0.1. Note that its peak, however, is clearly separated from the brightest part of the shell of G348.5+0.1.

5. The 90 cm VLA map shows significant curvature of the "jet" which is reminiscent of a partial shell and the "interior" of this new "shell" has significant low surface brightness emission much like the partial shells of G348.5+0.1 and G348.7+0.3. Note that a faint extension of emission on the northeastern part of the shell of G348.5+0.1 near $\alpha = 17^h11^m20^s$, $\delta = -38°24'$ might be a part of the new "shell" where it exits its superposition on the bright shell of G348.5+0.1. Evidence for this emission can also be found on our 20 cm map presented below.

Even this purely morphological examination suggests that the "jet" is not a component of G348.5+0.1 but defines the southern/southwestern rim of a third, partial shell SNR superposed on the G348+0 complex. The following higher resolution maps and discussion of the available spectral index information in the next section also support this hypothesis.

3.2. 20 *Centimeter Observations*

Our 20 cm VLA map is shown in Figure 2. Since the primary beam is only ∼30′, the map principally shows the region associated with G348.5+0.1 and the "jet." Figure 2 confirms the general morphology of G348.5+0.1 and the "jet" seen in our 90 cm map, but the increased resolution provides much better detail.

The 20 cm map shows much more clearly the curvature of the "jet" into a nearly completed shell, and the apparent distortion of the shell of G348.5+0.1 near $\alpha = 17^h11^m20^s$, $\delta = -38°24'$ as was seen on the 90 cm map. The higher resolution observations thus confirm the morphological arguments for an interpretation of the "jet" as a new, previously unidentified shell SNR rather than an extension from G348.5+0.1. Thus, henceforth we refer to the "jet" as the new SNR G348.5−0.0. This interpretation is further supported by spectral index arguments given in § 4 below.

Figure 2 also shows the "blown-out" region of the southwestern part of G348.5+0.1 in much more detail. This region of low surface brightness extends over a large area and is reminiscent of the highly asymmetric partial shells seen in better known Galactic SNRs such as VRO 42.05.01 (see Pineault, Landecker, & Routledge 1987 and references therein), IC 443, and Puppis A (see Erickson & Mahoney 1985 and references therein). Milne et al. (1988) have also reported similar "blowouts" in SNR G316.3−0.0 and SNR G332.4+0.1.

We note an enhanced ridge of emission on the southeastern edge of the "blowout" near $\alpha = 17^h11^m05^s$, $\delta = -38°36'$ which suggests that G348.5+0.1 is expanding into a region of higher density in the ISM on its southeastern side.

3.3. 6 *Centimeter Observations*

Our 6 cm map (Fig. 3) has the most limited field of view due to its primary beam of ∼9′ and thus shows only the intersection between G348.5−0.0 (formerly the "jet") and the eastern edge of G348.5+0.1. This map again shows the curvature of G348.5−0.0 and, if it is considered a partial shell, slight evidence for low surface brightness emission from the interior of this shell. Figure 3 also delineates the separation of

TABLE 2

FLUX DENSITY MEASUREMENTS FOR COMPONENTS OF THE G348+0 COMPLEX

FREQUENCY (MHz)	FLUX DENSITY (Jy)					
	G348.7+0.3		348.5−0.0 ("Jet")		G348.5+0.1	
	Value	Reference	Value	Reference	Value	Reference
80.0.....	46.0 ± 12.0	1	...	...	107.0 ± 10.7	1
	35.4	2	...	...	110.6 ± 16.6	12
160.0.....	40.7	2	...	...	108.0 ± 11.9	1
	47.0 ± 15.0	1	...	...	77.5	2
333.0.....	55.2 ± 2.9	3	>20.4	3	122.6 ± 6.2	3
408.0.....	40.6 ± 6.1	4	...	...	94.1	13
1410.0.....	39.8 ± 4.0	5	...	...	75.5 ± 7.6	5
1415.0.....	>28.0[a]	6	>9.0	6	>50.0	6
1443.0.....	>8.0b	3	>6.2	3	>45.6	3
2650.0.....	28.8 ± 2.9	5	...	...	52.5 ± 5.3	5
	21.2	7	...	...	45.5	7
2695.0.....	21.8 ± 0.4	8	...	...	37.6 ± 0.4	8
4835.0.....	...	...	>2.0	3	...	...
5000.0.....	14.4 ± 0.4	8	...	...	40.7 ± 4.1	10
	33.3	9	...	...	44.7	9
	22.9 ± 2.3	10	...	...	27.7 ± 0.3	8
8800.0.....	20.1	11	...	...	29.9	11
14700.0.....	18.4[b] ± 5.8	6	...	...	17.5 ± 5.1	6

[a] Includes a contribution of ~7.8 Jy from what is considered the "bridge" feature by Milne et al. 1979.

[b] Includes a contribution of ~10.7 Jy from what is considered the "bridge" feature by Milne et al. 1979.

REFERENCES.—(1) Dulk & Slee 1975; (2) Slee 1977; (3) This paper; (4) Kesteven 1968; (5) Milne & Hill 1969; (6) Milne et al. 1979; (7) Beard et al. 1969; (8) Altenhoff et al. 1970; (9) Milne & Dickel 1975; (10) Milne 1969; (11) Dickel et al. 1973; (12) Slee & Higgins 1973; (13) Green 1974.

G348.5−0.0 from the eastern shell of G348.5+0.1. This map indicates why previous observations made at lower resolution tended to blend these two separate sources into one, giving the impression of a "jet" emerging from G348.5+0.1.

The available flux densities from our VLA observations and from the literature are gathered in Table 2. All measurements have been brought to the Baars et al. (1977) flux density scale by using the correction factors tabulated by Kassim (1989a).

3.4. *Observations at Other Frequencies*

Observations of the G348+0 complex were made at 57.5 MHz (Kassim 1987, 1988) using the CLRO TPT telescope (Erickson, Mahoney & Erb 1982). For comparison purposes, we reproduce the CLRO 57.5 map of the field in Figure 5. Because of the limited resolution (~7 × 17′ FWHM), the entire complex of the SNRs G348.5−0.0, G348.5+0.1, and G348.7+0.3 are blended together. However, Kassim (1987) noted that the integrated flux density of 580±150 Jy at 57.5 MHz was "too high" by more than a factor of 2 in relation to the expected value of ~230 Jy extrapolated from higher frequency measurements of G348.5+0.1 and G348.7+0.3. (See the catalog by Green 1988 for earlier estimates of the spectra of these sources.) The additional, low surface brightness, extended emission seen in our new observations of the complex nicely explains this difference (see also § 4.4).

4. INDIVIDUAL SOURCE SPECTRA

These new observations make it possible to reconcile the "high" flux density measured at 57.5 MHz with the continuum spectra of each of the sources in the complex. It is immediately apparent from examination of Figures 1 and 2 that the most likely sources of this low-frequency excess are the diffuse emission associated with the southwestern part of G348.5+0.1, the northeastern part of G348.5−0.0, and from both the western and southeastern parts of G348.7+0.3. All three appear to have been partially or completely undetected by most other observers (see, e.g., Fig. 4 and Milne et al. 1979). We can proceed by estimating the high-frequency ($\nu \geq 333$ MHz) continuum spectra for each of the major features in the complex

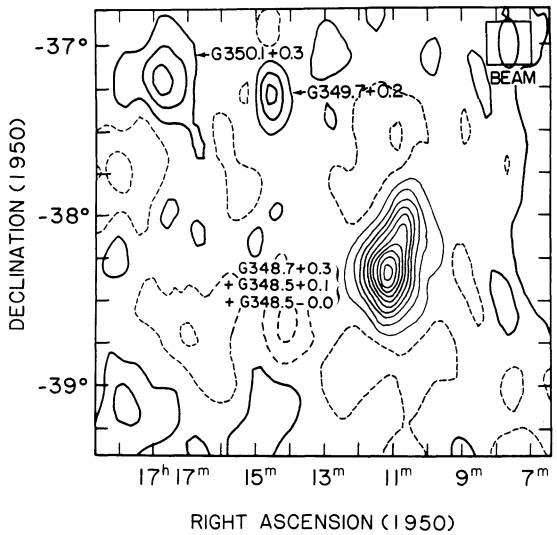

FIG. 5.—57.5 MHz Clark Lake map of the G348+0 SNR complex. The synthesized beam is 7′ × 17′ FWHM and is shown at the upper right. All features of the complex, G348.7+0.3, G348.5+0.1, and G348.5−0.0 (formerly the "jet"), are blended together into a single feature at this resolution. The contour levels are at −27, −9, 9, 27, 45, 63, 81, 99, 117, 135, 153, 171) × 1 Jy beam^{-1} with a peak brightness of 179 Jy beam^{-1}.

and then extrapolating them down to 57.5 MHz.[5] These extrapolated values can then be summed to compare with the integrated flux density measured by CLRO at 57.5 MHz.

4.1. *Spectrum of G348.7+0.3*

As discussed in § 3.1 above, we feel the morphology of the complex revealed in our new 90 cm VLA map favors an interpretation of the "bridge" emission as part of the SNR G348.7+0.3, rather than as a connection between this SNR and G348.5+0.1. Thus, to derive the spectrum of G348.7+0.3, we combine flux densities from the literature with our 90 cm flux density (all listed in Table 2) which includes the contribution from both the "bridge" and the main part of the SNR. For the measurements by Milne et al. (1979) at 1415.0 MHz (>28.0 Jy) and at 14,700.0 MHz (18.4 Jy), we use the sum of the flux densities they list for the SNR and the bridge component, as they considered these separately in their paper.

The derived spectrum is shown in Figure 6 where we have fitted a spectrum of constant index α ($S\alpha\nu^{+\alpha}$) from the flux densities listed in Table 2 and obtain a value of $\alpha = -0.3 \pm 0.1$.[6] Note that points observed at 80 and 160 MHz made using the Culgoora radio-heliograph (Dulk & Slee 1975; Slee 1977; Slee & Higgins 1973) have not been included since our 90 cm map reveals that both G348.5+0.1 and G348.7+0.3 have structure greater than 15′–20′ in size which would have been resolved out by Culgoora. The resultant spectrum is a typical one for a Galactic SNR and provides a satisfactory fit to the data.

4.2. *Spectrum of G348.5−0.0*

Table 2 also lists the best available flux densities for G348.5−0.0. Unfortunately, it is difficult to deduce anything but a crude lower limit to its spectral index since all previous observations above 1 GHz, including our own at 6 and 20 cm, resolve out a great deal of its flux density. However, if we compare the flux density of only the brightest part of the "jet" from the FST 1415 MHz map (>9.0 Jy; Milne et al. 1979) with the same portion of the source seen in our similar resolution 333 MHz VLA map (15.4 Jy) we can estimate a spectral index limit $\alpha \geq -0.4 \pm 0.1$.

Such a spectral index limit, while not definitive, does show that the G348.5−0.0 has a spectrum which is consistent with that expected for a Galactic SNR. Because the spectral data is so limited, it is only presented in Table 2 and not shown as a figure.

[5] Kassim 1989b has shown that, in the absence of thermal absorption which does not appear to be present here, SNRs show power-law spectra of constant index down to the lowest observable frequencies.

[6] Points which are only lower limits are not used to derive any of the spectra we present. However, we show them as arrows on both Figs. 6 and 7.

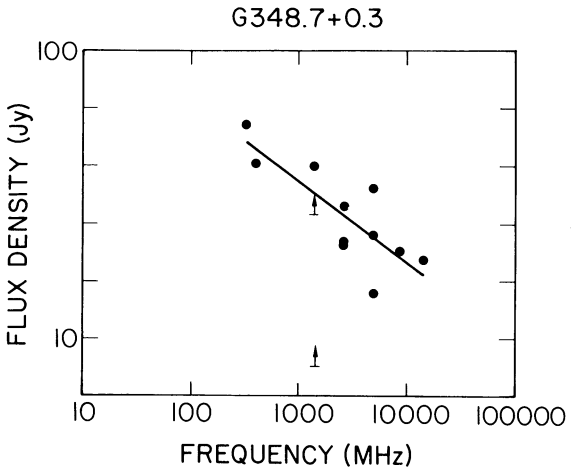

FIG. 6.—Radio continuum spectrum of G348.7+0.3. Data are taken from observations presented in this paper (Table 2) and from the literature. All flux densities have been brought to the Baars et al. (1977) flux density scale based upon conversion factors tabulated in Kassim (1988a). The straight line shows a spectrum of index $\alpha = -0.3$ obtained from a least-squares fit to the data.

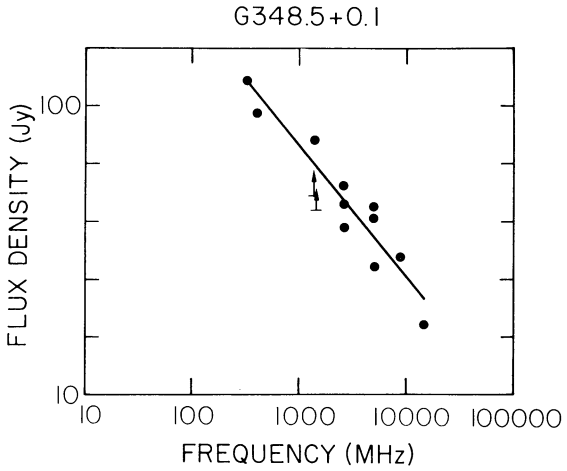

FIG. 7.—Radio continuum spectrum of G348.5+0.1. Data are taken from observations presented in this paper (Table 2) and from the literature. All flux densities have been brought to the Baars et al. (1977) flux density scale based upon conversion factors tabulated in Kassim (1988a). A spectrum of index $\alpha = -0.5$ (*straight line*) fits the data points well.

4.3. *Spectrum of G348.5+0.1*

All available flux density measurements for G348.5+0.1 are also gathered in Table 2, and the derived spectrum along with the data are plotted in Figure 7. A spectrum of constant index fit to these values yields $\alpha = -0.5 \pm 0.1$, again an average value for an SNR. As can be seen, the spectrum shown in Figure 7 provides a satisfactory fit to the available data. Errors in the derived spectra for both G348.7+0.3 and G348.5+0.1 result mainly from the scatter in measurements made at higher frequencies, probably reflecting error in or lack of detection of the low-level extended emission revealed in our 90 cm VLA map.

4.4. *Low-Frequency Spectrum of the G348+0 Complex*

We now extrapolate the expected flux density of the entire G348+0 complex to 57.5 MHz based on the spectral index estimates given in §§ 4.1–4.3 above and compare this result with the CLRO measured value presented in § 3.4. To do this we use the spectral index estimates for G348.5+0.1, G348.7+0.3, and G348.5−0.0 together with our 90 cm integrated flux densities listed in Table 2. We anchor these extrapolations to our new 90 cm VLA data because (1) we feel that the new 90 cm values are the most accurate currently available and (2) they are the closest in frequency to the CLRO measurements so that extrapolations should be less sensitive to errors in the derived spectral indices. In this way we estimate from our new 90 cm data an integrated flux density at 57.5 MHz of 430+80 Jy. This estimate agrees, within the expected errors, to the CLRO measured value of 580+150 Jy.

Since inclusion of the low surface brightness components in

the new spectral index determination removes an apparent deficit in the flux density for the complex when extrapolated from previously available high frequency measurements, we conclude that the poor brightness sensitivity of previous measurements was the origin of the apparent discrepancy. We are also now able to establish for the first time a consistent set of spectral index determinations for the three SNRs in the G348+0 complex.

5. CONCLUSIONS

We have presented observations at 6, 20, and 90 cm of the unusual SNR complex located near $l = 348°$, $b = 0°$. These observations were motivated by (1) an unusually "high" 57.5 MHz flux density for the complex, (2) a remarkable "jet" feature apparently extending from the eastern shell of the SNR G348.5+0.1, and (3) an apparent "bridge" of emission between the two SNRs G348.5+0.1 and G348.7+0.3.

Our new higher resolution, higher brightness sensitivity VLA observations allow us to study the complex in much more detail. From these, and also using existing observations from the literature, we conclude the following:

1. The "jet" feature in the complex is not associated with G348.5+0.1 but is a separate SNR showing a typical partial shell structure and having a typical spectral index $\alpha \sim -0.4$. This new SNR is designated G348.5−0.0 according to the usual convention. G348.5−0.0 may be physically associated with other members of the complex or may be simply superposed along the line of sight, we have no way of distinguishing in the present work.

2. G348.5+0.1 is larger than previously realized with a significant area of "blown-out" emission of very low surface brightness on its southwestern side. This asymmetric structure is similar to the morphology exhibited by a number of other large shell-type SNRs (e.g., VRO 42.05.01 and IC 443) and presumably indicates that it is expanding in a region of the ISM with significant large-scale density inhomogeneities. This extended, low surface brightness emission was not detected by most previous, higher frequency observations, and its integrated flux density helps account for part of the "excess" flux density seen by the earlier CLRO 57.5 MHz measurement.

3. The "bridge" of emission located between G348.5+0.1 and G348.7+0.3 is clearly detected but appears to form more of a faint extension to G348.7+0.3, with which it is clearly connected, than a physical connection to G348.5+0.1. Thus we conclude that it is part of the SNR G348.7+0.3. As with the SNR G348.5−0.0, there is no evidence that G348.7+0.3 is physically associated with other members of the complex and may simply be superposed along the line of sight.

We thank C. O'Dea for useful comments and discussions. Partial support for this work was provided by NASA through grant HF-1001, 01-90a awarded by the Space Telescope Science Institute which is operated by Associated Universities for Research in Astronomy Inc. for NASA under contract NAS5−2655s.

REFERENCES

Altenhoff, W. J., Downes, D., Good, L., Maxwell, A., & Rinehart, R. 1970, A&AS, 1, 319
Baars, J. W. M., Genzel, R., Pauliny-Toth, I. I. K., & Witzel, A. 1977, A&A, 61, 99
Beard, M., Thomas, B. M., & Day, G. A. 1969, Australian J. Phys., Ap. Suppl., 12, 27
Dickel, J. R., Milne, D. K., Kerr, A. R., & Ables, J. G. 1973, Australian J. Phys., 26, 370
Downes, A. 1984, MNRAS, 210, 845
Dulk, G. A., & Slee, O. B. 1975, ApJ, 199, 61
Erickson, W. C., & Mahoney, M. J. 1985, ApJ, 290, 596
Erickson, W. C., Mahoney, M. J., & Erb, K. 1982, ApJS, 50, 403
Green, A. J. 1974, A&AS, 18, 267
Green, D. A. 1988, Ap&SS, 148, 3
Kassim, N. E. 1987, Ph.D. thesis, University of Maryland
———. 1988, ApJS, 68, 715
Kassim, N. E. 1989a, ApJS, 71, 799
———. 1989b, ApJ, 347, 915
Kesteven, M. J. L. 1968, Australian J. Phys., 21, 369
Milne, D. K. 1969, Australian J. Phys., 22, 613
Milne, D. K., Caswell, J. L., Kesteven, M. J., Haynes, R. F., & Roger, R. S. 1988, in Lecture Note in Physics, Vol. 316, Supernova Shells and Their Birth Events, ed. Wolfgang Kundt (Heidelberg: Springer), p. 98
Milne, D. K., & Dickel, J. R. 1975, Australian J. Phys., 28, 209
Milne, D. K., Goss, W. M., Haynes, R. F., Wellington, K. J., & Caswell, J. L. 1979, MNRAS, 188, 437
Milne, D. K., & Hill, E. R. 1969, Australian J. Phys., 22, 211
Napier, P. J., Thompson, A. R., & Ekers, R. D. 1983, Proc. IEEE, 71, 1295
Pineault, S., Landecker, T. L., & Routledge, D. 1987, ApJ, 315, 580
Slee, O. B. 1977, Australian J. Phys. Ap. Suppl., 43, 1
Slee, O. B., & Higgins, C. S. 1973, Australian J. Phys. Ap. Suppl., 27, 1